



HAL
open science

Antibiotic tolerance and degradation capacity of the organic pollutant-degrading bacterium *Rhodococcus biphenylivorans* TG9T

Chungui Yu, Jean Armengaud, Ryan Andrew Blaustein, Kezhen Chen, Zhe Ye, Fengjun Xu, Jean-Charles Gaillard, Zhihui Qin, Yulong Fu, Erica Marie Hartmann, et al.

► **To cite this version:**

Chungui Yu, Jean Armengaud, Ryan Andrew Blaustein, Kezhen Chen, Zhe Ye, et al.. Antibiotic tolerance and degradation capacity of the organic pollutant-degrading bacterium *Rhodococcus biphenylivorans* TG9T. *Journal of Hazardous Materials*, 2021, 424, pp.127712. 10.1016/j.jhazmat.2021.127712 . hal-04460321

HAL Id: hal-04460321

<https://hal.science/hal-04460321>

Submitted on 15 Feb 2024

HAL is a multi-disciplinary open access archive for the deposit and dissemination of scientific research documents, whether they are published or not. The documents may come from teaching and research institutions in France or abroad, or from public or private research centers.

L'archive ouverte pluridisciplinaire **HAL**, est destinée au dépôt et à la diffusion de documents scientifiques de niveau recherche, publiés ou non, émanant des établissements d'enseignement et de recherche français ou étrangers, des laboratoires publics ou privés.



Contents lists available at ScienceDirect

Journal of Hazardous Materials

journal homepage: www.elsevier.com/locate/jhazmat

Research Paper

Antibiotic tolerance and degradation capacity of the organic pollutant-degrading bacterium *Rhodococcus biphenylivorans* TG9^T

Chungui Yu^a, Jean Armengaud^c, Ryan Andrew Blaustein^b, Kezhen Chen^a, Zhe Ye^a, Fengjun Xu^a, Jean-Charles Gaillard^c, Zhihui Qin^a, Yulong Fu^a, Erica Marie Hartmann^{b,*}, Chaofeng Shen^{a,*}

^a Zhejiang University, Department of Environmental Engineering, College of Environmental and Resource Sciences, Hangzhou 310058, Zhejiang, China

^b Department of Civil and Environmental Engineering, Northwestern University, Evanston, IL, USA

^c Université Paris-Saclay, CEA, INRAE, Département Médicaments et Technologies pour la Santé (DMTS), SPI, F-30200 Bagnols-sur-Cèze, France

ARTICLE INFO

Editor: Dr Shaily Mahendra

Keywords:

Antibiotic tolerance
Degradation
Organic pollutants
Rhodococcus
Proteomics

ABSTRACT

Antibiotics are ubiquitous in soil due to natural ecological competition, as well as emerging contaminants due to anthropogenic inputs. Under environmental factors like antibiotic stress, some bacteria, including those that degrade environmental pollutants, can enter a dormant state as a survival strategy, thereby limiting their metabolic activity and function. Dormancy has a critical influence on the degradative activity of bacteria, dramatically decreasing the rate at which they transform organic pollutants. To better understand this phenomenon in environmental pollutant-degrading bacteria, we investigated dormancy transitions induced with norfloxacin in *Rhodococcus biphenylivorans* TG9^T using next-generation proteomics, proteogenomics, and additional experiments. Our results suggest that exposure to norfloxacin inhibited DNA replication, which led to damage to the cell. Dormant cells then likely triggered DNA repair, particularly homologous recombination, for continued survival. The results also indicated that substrate transport (ATP-binding cassette transporter), ATP production, and the tricarboxylic acid (TCA) cycle were repressed during dormancy, and degradation of organic pollutants was down-regulated. Given the widespread phenomenon of dormancy among bacteria involved in pollutant removal systems, this study improves our understanding of possible implications of antibiotic survival strategies on biotransformation of mixtures containing antibiotics as well as other organics.

1. Introduction

Antibiotics are naturally occurring in the soil and play important roles in ecological competition. In addition, human-made antibiotics have increasingly accumulated in the environment (e.g., soil and water) due to widespread consumption, high fraction of un-metabolized drug, and unregulated discharge (Klein et al., 2018). Anthropogenic antibiotic residues in the environment pose health and environmental problems worldwide (Levy and Marshall, 2004; Klein et al., 2018), becoming a global concern (Neu, 1992; Meredith et al., 2015; Meng et al., 2016; Viancelli et al., 2020). Antibiotic resistance and tolerance, which are common in soil-dwelling microorganisms as natural survival strategies for harsh and complex environments, are a major threat (Lewis and Shan, 2017; Pu et al., 2019). Antimicrobial-resistant organisms can grow in the presence of an inhibitory concentration of antibiotic. Many studies

focus on pathogens and the risks they present to human health (Levy and Marshall, 2004; Baker et al., 2018), though environmental non-pathogens encode many antibiotic resistance genes as well (Zhu et al., 2013; Tymensen et al., 2019). Antibiotic tolerance is a genetically indistinguishable, spontaneous phenotypic switch within a small subset of a microbial population (Brauner et al., 2016; Lewis and Shan, 2017). While antibiotic tolerance is a less critical direct threat to human health than resistance, understanding this mechanism in environmental bacteria is extremely relevant to environmental health.

In addition to emerging contaminants like antibiotic residues (Baker et al., 2018; Viancelli et al., 2020), many environments are highly contaminated with traditional pollutants such as heavy metals or organics including polychlorinated biphenyls and polycyclic aromatic hydrocarbons (Adriaens and Focht, 1990; Louvado et al., 2015). Bioremediation is an important process in the degradation of environmental

* Corresponding authors.

E-mail addresses: erica.hartmann@northwestern.edu (E.M. Hartmann), ysxzt@zju.edu.cn (C. Shen).

<https://doi.org/10.1016/j.jhazmat.2021.127712>

Received 28 June 2021; Received in revised form 14 October 2021; Accepted 3 November 2021

Available online 17 November 2021

0304-3894/© 2021 Elsevier B.V. All rights reserved.

pollutants, but varying environmental conditions have strong implications on the phenotypes of the bacteria involved in that process. Under unfavorable environmental conditions, microorganisms may enter a viable but non-culturable (VBNC) state. Such transitions have been reported for more than 68 bacterial species as well as several members of Archaea and Eukaryota (mainly fungi) (Pinto et al., 2015; Ayrapetyan et al., 2018). Non-sporulating bacteria that enter this dormant state remain viable with intact cell membranes, low metabolic activity, and inhibited growth, though they become cultivable when the surrounding conditions are once again favorable (Oliver, 1995; Whitesides and Oliver, 1997). Many factors are traditionally thought to limit degradation, like temperature, solubility/bioavailability of the pollutant, etc. In addition, there are many physical and chemical factors (e.g., nutrient deprivation, pH, radiation, other organic pollutants), specifically the presence of antibiotic pollution or antibiotics as competition, that influence dormancy (generally) and in turn, limit their degrading abilities (Oliver, 1995; Al-Bana et al., 2014). Given the rise in antibiotic pollution, investigating the dormant state in biodegradative bacteria is increasingly important, as antibiotic-induced dormancy could strongly influence degradation of other environmental contaminants. In this study, we seek to broaden our understanding of the potential impacts of antibiotics on organisms involved in the bioremediation of other organic pollutants.

Rhodococcus biphenylivorans TG9^T, is an intriguing model for understanding the role of antibiotic resistance and tolerance in dormancy-associated bacterial degradation. *R. biphenylivorans* TG9^T is a Gram-positive, aerobic, and rod-coccus shaped actinobacteria. The strain can use at least 14 types of organic pollutants as sole source of carbon/energy, notably including biphenyl and polychlorinated biphenyl (PCB) (Yu et al., 2021). It was originally isolated from organic pollutant-contaminated sediment following recovery from the dormant state via exposure to resuscitation-promoting factor (Rpf) protein (Su et al., 2015). The genome of TG9^T has many predicted antibiotic resistance genes (i.e., TG9^T is resistant to gentamicin and streptomycin, rifampin, tetracycline, chloramphenicol, and polymyxin as presented by Yu et al., (Yu et al., 2021)), indicating the potential for survival in antibiotic-contaminated environments. However, if instead of adopting a resistance phenotype, the strain were to switch to tolerance, it would enter dormancy to survive and only resuscitate when the conditions become favorable. Transitions into a dormant state can be induced in TG9^T in vitro via a chemical stressor such as norfloxacin, which inhibits the replication of DNA and is associated with the growth and activity of cells (Shen and Pernet, 1985; Hsu et al., 2006). It is a fluoroquinolone that has been used for decades in medicine and has additional applications in aquaculture (Liu et al., 2017; Zhang et al., 2021; Wang et al., 2021). As a pollutant, norfloxacin also poses a threat to human and environmental health (Le et al., 2005; Boonsaner and Hawker, 2010; Meng et al., 2016; Ryu et al., 2019; Xie et al., 2019).

Here, we use norfloxacin as a representative antibiotic of environmental concern to illustrate its impact on the phenotype and biphenyl degradation activity of *R. biphenylivorans* TG9^T. While multi-omics is of prime interest to understand how a biological system functions, here, we focused on proteomics as proteins are the workhorses of metabolism, nutrient transport, protein synthesis and the construction of cellular and extracellular edifices, thus consequently proteomics connects ideally genomic potential and metabolic information. We used next-generation proteomics, specifically tandem mass tagging (TMT), to characterize the molecular phenotype and identify key proteins involved in the response to stresses. Actively growing (control) cells, dormant cells and resuscitated cells were analyzed to determine what happens when an antibiotic interrupts metabolism in an organic pollutant-degrading bacterium, and changes in degradation potential were evaluated and validated. This research represents a new exploration of antibiotic-induced dormancy of a non-pathogenic pollutant-degrading bacterium. It expands our overall understanding of antibiotic resistance and tolerance, as well as dormancy-associated bacterial degradation of

organic pollutants.

2. Results

2.1. TG9^T response of norfloxacin treatment

2.1.1. The viability of TG9^T in three states

The global strategy deployed in this study was to investigate three distinct phenotypic states (Fig. 1). First, to assess changes in viability of TG9^T when it encounters norfloxacin, respiratory activity, cultivability and cell density were investigated (Fig. 1, Jia et al., 2020). Under the pressure of norfloxacin, the number of respiring cells (cells that have respiring activity) decreased to 10^5 cfu mL⁻¹ in the first 6 days and then remained unchanged, while the cells sharply became uncultivable in 5 days. After removing norfloxacin, the cells transitioned out of dormancy and regained cultivability in a time-dependent manner. In 34 h, the respiration activity and density of cells began to increase. After 58 h, the total cell, viable cell, cultivable cell numbers remained stable.

2.1.2. DNA replication inhibition

To identify the essential proteins involved when a chemical encounters a microbe, we used TMT to quantify and compare proteins in the un-treated control cells, norfloxacin-induced dormant cells and resuscitated cells (n = 3 biological replicates per treatment). In total, 3123 proteins were identified, of which 2942 proteins were quantified, and differentially abundant proteins between two states were analyzed (fold change over 1.2 or lower 1/1.2 and p value < 0.05) (Supplementary Fig. S1). We note that norfloxacin targets inhibition of DNA replication (Shen and Pernet, 1985; Hsu et al., 2006), and proteins related to this function had differential abundances across the three states (control, dormant, and resuscitated), such as helicase, DNA polymerase, ligase, gyrase, and single-stranded binding protein (Supplementary Table S1). Abundance of helicase was highest in the dormant and resuscitated cells. DNA polymerases such as DnaG and DnaB, DNA ligases such as LigD, and LigA decreased in the dormant cells compared with the controls. During the process of resuscitation, the abundance of DNA polymerase increased but was still lower than that of the control. The abundance of DNA gyrase subunit B (GyrB) followed the order of dormant > resuscitated > control. Dormant cells had the highest abundance of single-stranded DNA-binding protein, followed by resuscitated, and control. Thus, as expected, protein production related to the DNA replication pathway underwent significant changes during the process of transitioning in and out of dormancy. The inhibition of DNA replication might lead to DNA damage of the current cell, and also repress cell division and production of new cell generation. Such norfloxacin targeted damages, along with non-targeted stress, reduce metabolic activity of the cell, resulting in transitions to a dormant state for survival.

2.1.3. DNA repair pathway

As DNA replication was interrupted, exposed DNA was susceptible to damage and DNA repair becomes essential. As such, dormant cells need to repair damaged DNA for survival. Several proteins involved in DNA repair pathways were significantly differentially abundant across the three states, including homologous recombination repair, base excision repair, nucleotide excision repair, mismatch repair, non-homologous end-joining repair and some other repair pathways (Fig. 2). Among them, the most significantly enriched pathways were homologous recombination repair and base excision repair.

The related proteins of control, dormant and resuscitated cells were annotated on the homologous recombination repair pathway (Fig. 2A). Many proteins involved in this pathway had higher abundance in dormancy than the other two states (control, resuscitated). RecA had the largest fold difference (dormant/control, 4.5), along with single-stranded binding protein SSB (dormant/control, 2.35) and RecX (dormant/control, 1.40). RecA is one of the essential proteins related to

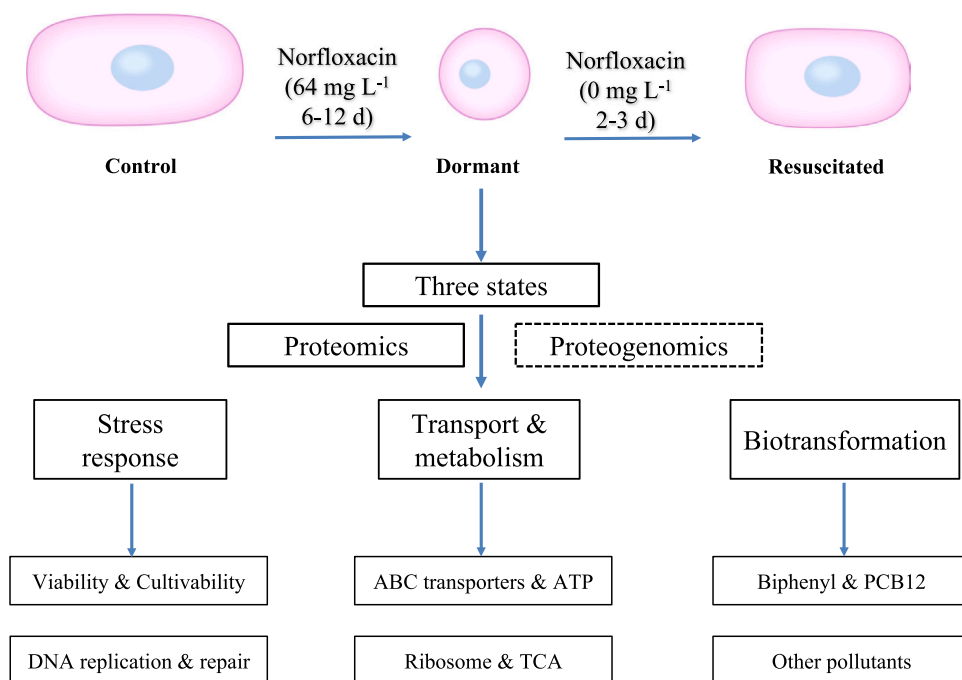


Fig. 1. Experiment and analysis setup. The three states of strains were prepared as follows. Control cells were those without treatment of norfloxacin. Dormant cell was induced under a final concentration of 64 mg L^{-1} norfloxacin for 6–12 days. Cell resuscitation was conducted by removing norfloxacin and resuspending cell pellet in fresh media for 72 h of culture. The three states of samples were analyzed using proteomics and proteogenomics, which focused on stress response, function difference, transport and metabolism.

homologous recombination repair. The sequence of RecA from TG9^T was blasted through NCBI tool BLAST and found to be unique (<https://blast.ncbi.nlm.nih.gov/Blast.cgi/20200820>). Only RecA from *Mycobacterium smegmatis* was found to share 93% sequence identity. Properties of RecA, including its tertiary structure, were predicted with SWISS-MODEL (Fig. 2C). The RecA monomer consisted of a central domain, which comprised P-loop, L1 and L2 loop involved in nucleotide and DNA binding. Its domain was predicted to be flanked by two smaller domains, a conformation which is different from that of RecA from *M. smegmatis*. These results underscore the need for homologous recombination repair under damage from norfloxacin treatment, and suggest that RecA may be more important than other proteins related to homologous recombination repair in TG9^T.

2.2. Substrate import and energy metabolism

To fit into our overall understanding of what happens when strain TG9^T encounters norfloxacin, protein-protein interactions were predicted from co-occurrence patterns of proteins and pathways in the three states. As for protein-protein interactions, sequences of differentially produced proteins of the three compared groups (dormant/control, resuscitated/control and resuscitated/dormant cells) were searched against the STRING database (version 11.0). Interactions with a high confidence score > 0.7 , and the top 100 highest degree network of protein nodes were displayed in Cytoscape (Fig. 3, Supporting Table S3). The greater the degree, the more proteins it putatively associates with, indicating that the protein is more important in the network.

Predicted protein-protein interactions indicated down-regulation of metabolic activity. First, under the stress of norfloxacin, the strain might trigger an inhibition of ATP-binding cassette transporter (ABC transporter) pathway to halt continuing damage. ABC transporters responsible for transport of substrate, including general ABC transporters, and transport of specific substrates such as nitrate, iron, biotin, heme, phospholipid/cholesterol/gamma-HCH, sorbitol/mannitol, manganese, and glutamate, were down-regulated in dormant/control and up-regulated in resuscitated/dormant cells (Supporting Table S3). Next, ATP production might be repressed. The inhibition of ABC transporter systems might inhibit the uptake of extracellular materials such as norfloxacin, biphenyl and PCB12, and nutrients moving into the cell. As

a result, the toxicity of the norfloxacin would become lower, but the cell would lack exogenous nutrients. ATP-dependent proteins, such as cation-transporting ATPase, ATP-dependent 6-phosphofructokinase, ATP-dependent Clp protease, ATP-dependent DNA helicase and ATP-dependent DNA ligase, decreased in the dormant/control group of protein-protein interactions. As cells need intracellular energy for survival, we found the abundance of some proteins involved in energetic metabolism to become increased when entering into dormancy and then decreased upon leaving. These proteins mainly had functions related to production and hydrolysis of ATP, catalytic activity of alanine-synthesizing transaminase, glutamate 5-kinase and peptidyl-tRNA hydrolase, phosphoprotein and ammonium transmembrane transporter activity. The ATP concentrations in control, dormant and resuscitated cells were tested (Fig. 4, the standard curve was $y = 0.000009x - 0.015$, $R^2 = 0.99$). There was a decrease of ATP production by dormant cells when compared with the control cells, which was consistent with the produce of the energy proteins. Moreover, lack of ATP might also slow down the translation process. The ribosome pathway had the greatest degree of connectivity in the protein-protein interaction analysis, which suggested inhibition of protein synthesis (Fig. 3). Almost all the ribosomal proteins, including 30 S and 50 S ribosomal proteins were differentially abundant (Supporting Table S2). Except for 50S ribosomal protein L7, L9, L33 and 30S ribosomal protein S1, S2, S3, most of the ribosomal proteins first decreased when entering dormancy (dormant/control), then increased when transitioning out of dormancy (resuscitated/dormant, resuscitated/control).

2.3. Degradation capacity in control, dormant and resuscitated TG9^T

2.3.1. Biphenyl and PCB degradation

The degradation activity of the control, dormant and resuscitated cells was tested to evaluate the influence of chemicals on how environmental microbes function. Briefly, cells were collected, washed, resuspended, and cultured in mineral salt medium with either 1500 mg L^{-1} biphenyl or 50 mg L^{-1} 3,4-dichlorobiphenyl (PCB12) as the carbon source. The degradation rate of biphenyl and PCB12 was then detected over time. The original cell densities were similar, and the dormant cells were successfully resuscitated during culturing. For degradation of biphenyl during 12 and 60 h, the degradation rate of

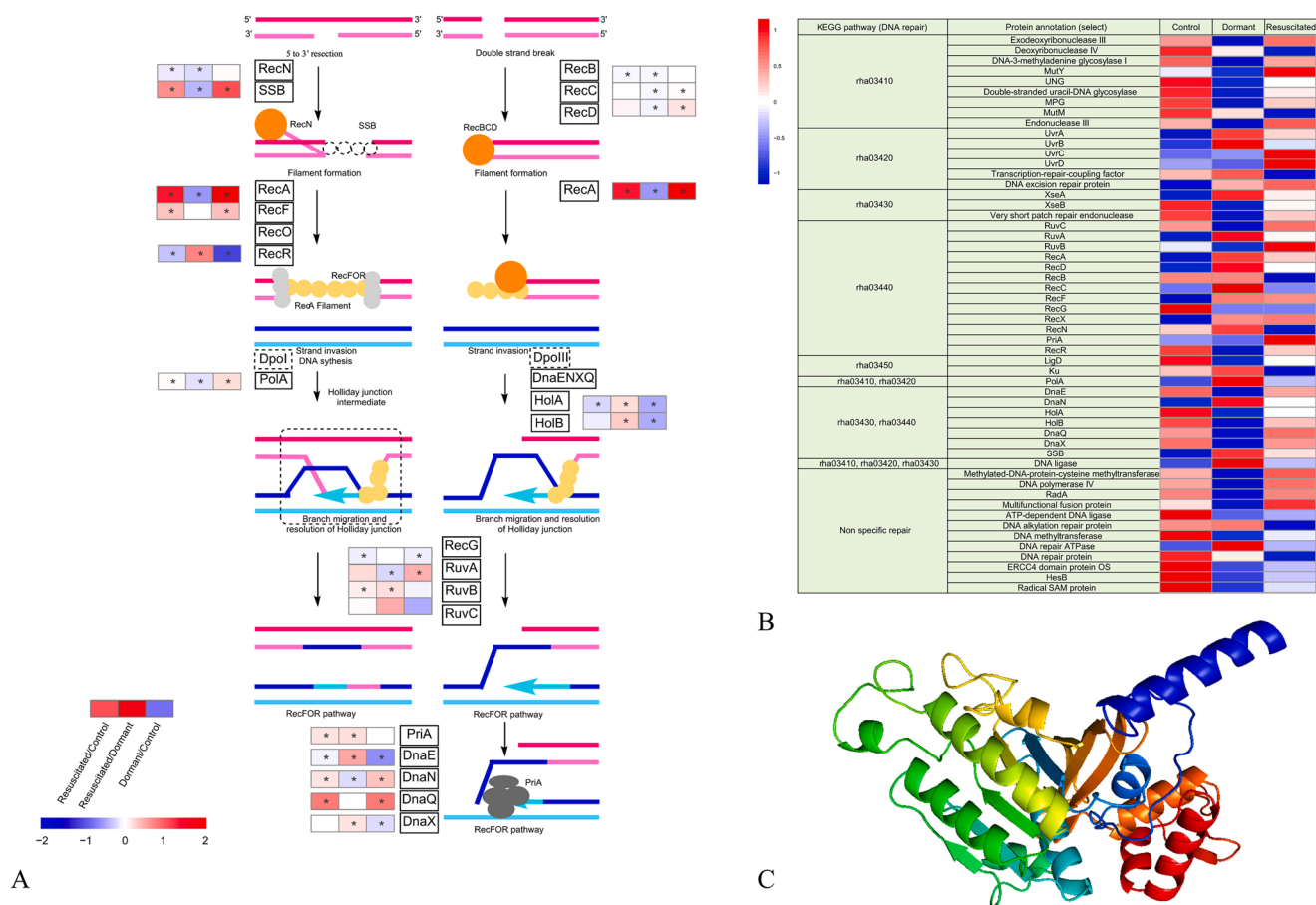


Fig. 2. DNA repair related proteins in control, dormant and resuscitated cell. (A) Differentially produced proteins of homologous recombination repair. (B) Heatmap of differentially produced proteins related to DNA repair pathway in control, dormant and resuscitated cell. (C) Predicted tertiary structure of RecA protein of TG9^T. In A, the colorful rectangles represent heatmap of differentially produced proteins in the compared groups, including resuscitated/control, resuscitated/dormant and dormant/control from left to the right, respectively. And the * indicates that the production of proteins in the two groups show significantly difference. rha03410, base excision repair. rha03420, nucleotide excision repair. rha03430, mismatch repair. rha03440, homologous recombination repair. rha03450, non-homologous end-joining repair. In C, the structure of the protein RecA was predicted by SWISS-MODEL (<https://swissmodel.expasy.org>) and showed by PyMOL (v2.4.1).

control was higher than the dormant and resuscitated samples, and the degradation of dormant and resuscitated samples remained with little change in the first 36 h and then increased about 96% between 36 h and 60 h (Fig. 5A). As for degradation of PCB12, the degradation rate of control cells was much higher than the dormant and resuscitated sample throughout the experiment (Fig. 5B). The dormant and resuscitated samples showed a similar trend of degradation as for biphenyl, between 0 and 36 h, the degradation of PCB12 remained identical, after 36 h, the PCB12 degradation rate improved and remained with little change. The highest degradation rate of biphenyl and PCB12 was about 85% and 69% for control sample, respectively. The highest degradation rate of biphenyl and PCB12 was about 85% and 10% for dormant and resuscitated sample, respectively. The difference of degradation for rate biphenyl and PCB12 might be due to the difficulty in using chlorinated substrates as the sole carbon source, which might be even harder for dormant cells.

Enzymes in the Bph pathway that responsible for degradation of biphenyl and PCBs (i.e., BphA, BphB, BphC, BphD, BphH, BphI and BphJ) were identified in all TG9^T cell states (Fig. 5C). However, the abundances of most of these proteins decreased in dormant cells when compared with the control population. During the transition from dormancy to resuscitation, abundances of some Bph proteins increased (BphB, BphI2), while others slightly decreased. When comparing the resuscitated with the control cells, the abundance of all proteins was lower, except for BphB, which was significantly higher (resuscitated/

control = 1.45).

2.3.2. Degradation of organic pollutants in different states

Our previous work revealed that *R. biphenylivorans* TG9^T could use at least 14 pollutants as its sole carbon source, and genes involved in 20 xenobiotics biodegradation and metabolism pathways were annotated in its genome (Yu et al., 2021). Regarding the proteomic analysis, we observed differential abundance of proteins in the three states related to 14 pathways of xenobiotics biodegradation and metabolism, including the degradation of chlorocyclohexane and chlorobenzene, benzoate, fluorobenzoate, xylene, dioxin, toluene, naphthalene, atrazine, aminobenzoate, styrene, steroid, polycyclic aromatic hydrocarbons, chloroalkane and chloroalkene, and caprolactam (Supplementary Fig. S2). Among them, the most significantly enriched pathways were those responsible for degradation of benzene-ring pollutants such as biphenyl and PCBs. Other differentially abundant proteins were involved in fatty acid, geraniol, lysine, valine, leucine and isoleucine, limonene and pinene degradation, synthesis and degradation of ketone bodies, RNA degradation, and degradation of aromatic compounds (Supplementary Fig. S2).

Pollutants would finally be metabolized via the tricarboxylic acid (TCA) cycle. Proteins related to the TCA cycle were found to be significantly differentially abundant (Supplementary Table S4). The material of the first reaction of TCA, acetyl-CoA, was found to be down-regulated when transitioning into dormancy from active state (dormant/

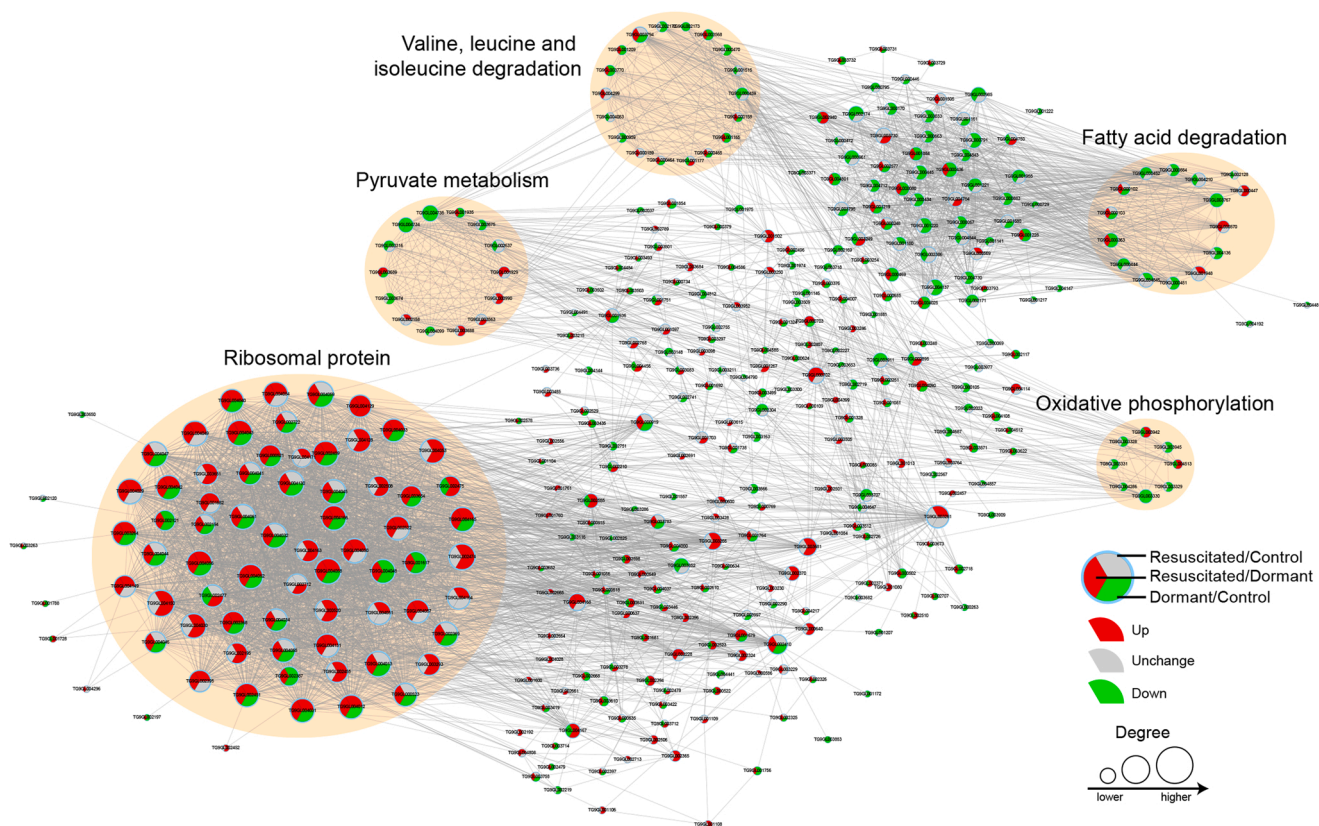


Fig. 3. Protein and protein interaction of differentially produced proteins in three states. Protein-protein interaction was conducted on STRING database (version 11.0) and visualized in Cytoscape (3.7.1) using all differentially produced protein sequences of three compared groups. We fetched all interactions that had a confidence score > 0.7 and displayed the network of protein nodes with top 100 highest degree.

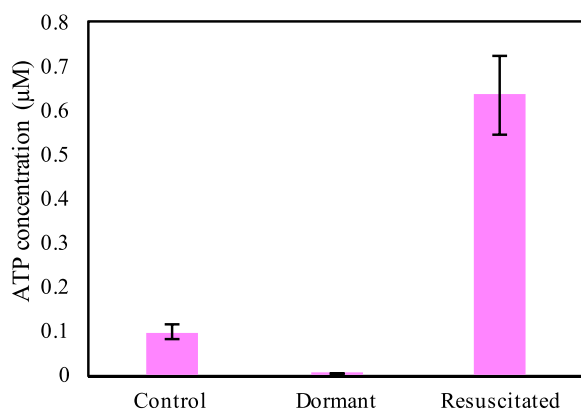


Fig. 4. ATP concentrations in control, dormant and resuscitated cells. The fluorescence values of each sample were corrected to the corresponding ATP concentration based on the standard curve ($y = 0.000009x - 0.015$, $R^2 = 0.99$).

control = 0.31, 0.41, 0.59, 0.62). Citrate synthase (dormant/control = 1.27; resuscitated/control = 1.28), isocitrate dehydrogenase (dormant/control = 1.16; resuscitated/control = 1.30), and malate dehydrogenase (dormant/control = 1.07; resuscitated/dormant = 1.50) were slightly increased, which indicated lack of ATP. Succinate dehydrogenase was decreased (dormant/control = 0.58). Other pathways related to the TCA cycle were also down regulated, including fatty acid degradation, lysine degradation, valine, leucine and isoleucine degradation, pyruvate metabolism, and oxidative phosphorylation, aspartate and glutamate metabolism. These results indicated that metabolism was mostly down-regulated in dormant cells.

2.4. Genome annotation of unique or interesting features using proteogenomics

We further leveraged the large proteomics dataset to improve the annotation of TG9^T genome using a proteogenomics strategy. These results supplement the existing genome annotation by revealing mis-annotated or previously unknown (e.g., “hypothetical protein”) features and functions of TG9^T. A systematic six-frame translation of all possible ORFs was performed to create a database for the proteogenomics search. Based on the identification of at least two novel peptides per translated ORF, we reported evidence for the presence of 72 additional coding sequences that were missed in terms of annotation in the first version of the annotated genome (Supplementary Table S5). One of these proteins is certified with 20 peptides and corresponds to a NfnB-like nitroreductase that catalyzes reduction of a variety of nitroaromatic compounds, including nitrofurans, nitrobenzenes, nitrophenol, and nitrobenzoate. Among these 72 mass spectrometry-certified novel proteins, 17 share sequence similarities with bacterial proteins until now annotated as hypothetical, but containing conserved structural domains not yet characterized in terms of function. This may explain why these genes were not called at the TG9^T annotation stage based on genomic sequence alone. Some of the newly annotated proteins are related to key functions, such as proteins related to the TCA cycle, including polysaccharide pyruvyl transferase family protein, glutamate-cysteine ligase, acetyl/propionyl/methylcrotonyl-CoA carboxylase subunit alpha and acetyl-CoA carboxylase subunit beta. Others are related to catabolism and degradation of pollutants, such as reductase, transferase, dehydratase, dehydrogenase, carboxylase, deaminase, desaturase, ammonia-lyase, thioesterase, peptidase, and type I restriction-modification endonuclease. As a result, our study was able to refine the genome annotation of *R. biphenylivorans* TG9^T, which is an important

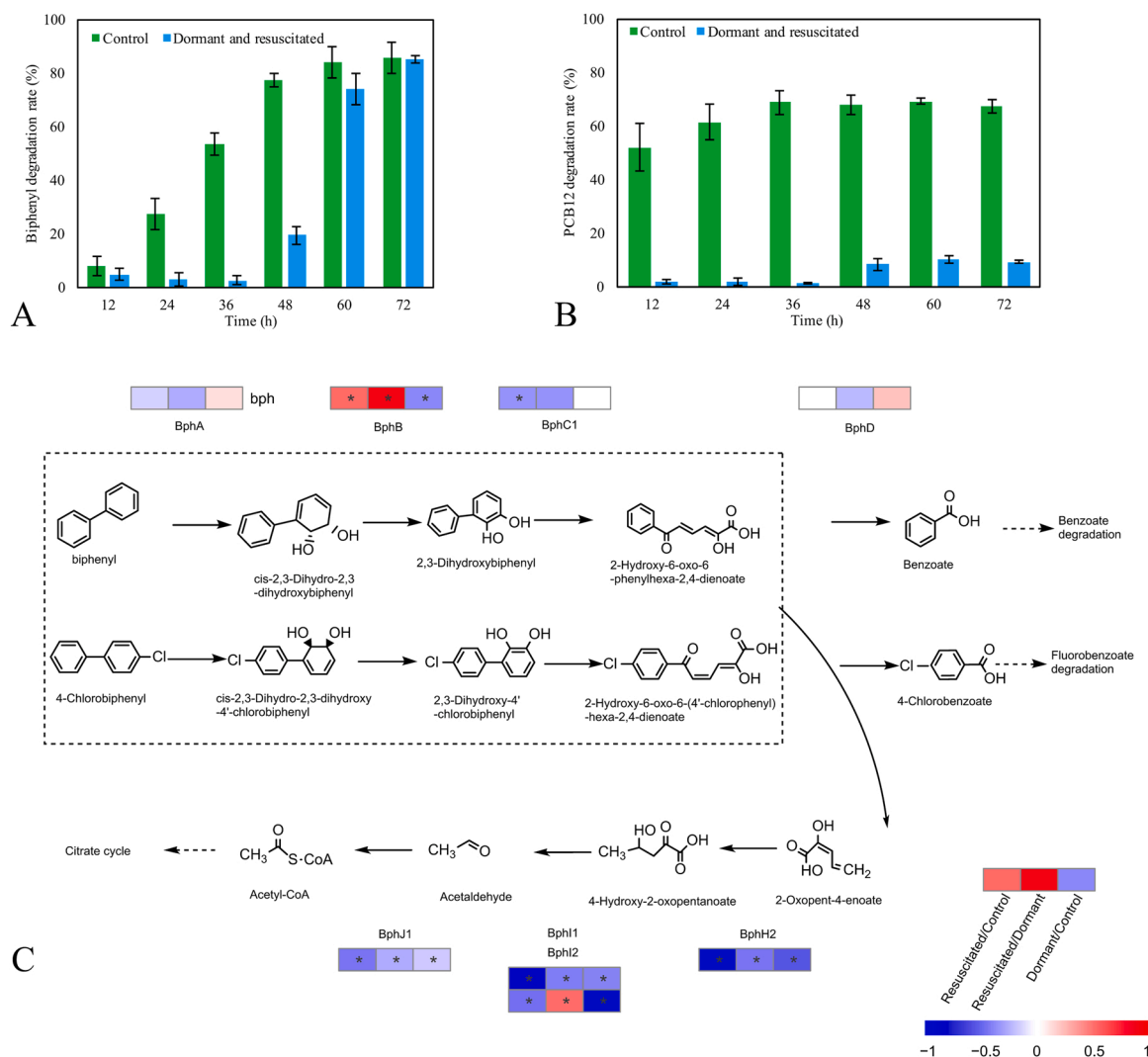


Fig. 5. Degradation related proteins in control, dormant and resuscitated cell. (A) Biphenyl degradation. (B) PCB12 degradation. (C) Differentially produced Bph proteins of biphenyl and PCB degradation. For degradation experiment, the control, dormant TG9^T were suspended in mineral medium (approximately 10⁵ cfu mL⁻¹). Biphenyl or PCB12 was added and the final set concentration was 1500 mg L⁻¹ and 50 mg L⁻¹ of biphenyl, and PCB12, respectively. The cap of the tubes was covered tightly to stop volatile. The controls were done the same as the samples, except replacing the active TG9^T solution with sterilized TG9^T culture. The degrading efficiency was showed as the difference between the reduction rate of the experimental group and the control group. In Fig. 5C, the colorful rectangles represent heatmap of differentially produced proteins in the compared groups, including resuscitated/control, resuscitated/dormant and dormant/control from left to the right, respectively. And the * indicates that the production of proteins in the two groups show significantly difference.

asset for future molecular studies with this model bacterium.

3. Discussion

To investigate survival strategies and functional transitions of an organic pollutant-degrading environmental bacterium, the antibiotic tolerance and degradation activity of *R. biphenylivorans* TG9^T were assessed using proteomics. Together with the previous genomic analysis showed that strain TG9^T had antibiotic resistance, dormancy and degradation related genes which were also core to *Rhodococcus* (Yu et al., 2021). Strain TG9^T might be a potential candidate of *Rhodococcus* for study on bacterial survival strategies and remediation of complex pollutants.

The present study improved our general understanding of bacterial survival strategies of bacteria. Bacterial survival in the natural environment is often dependent on enduring selective pressures via encoding relevant functional antibiotic resistance genes, and many non-pathogenic environmental bacteria encode features for multi-drug resistance in conserved export pathways (Blaustein et al., 2019; Dai

et al., 2021). When a particular strain is not resistant but tolerant to an antibiotic, subpopulations of the organism might enter dormancy to survive. Multiple antibiotics can induce bacterial dormancy. For instance, tetracycline, rifampicin, vancomycin and quinupristin could induce a VBNC state in *Staphylococcus epidermidis* and *Staphylococcus aureus* biofilms (Pasquaroli et al., 2013; Carvahais et al., 2018). Ampicillin was used to induce *Cronobacter sakazakii* into the VBNC state (Zhang et al., 2020). Bacterial antibiotic tolerance was monitored at the single-cell level and found that each individual survival cell shows different "dormancy depth" (Pu et al., 2019). When exposed to norfloxacin, DNA gyrase of DNA replication was repressed and a large number of dipolymer was produced. Exposed DNA was susceptible to damage, which decreased the metabolic activity of the viable cells. The production of new cells also slowed because of inhibition of cell division. For survival, dormant cells could activate the DNA repair system to correctly splice DNA fragments. We observed that many proteins related to DNA repair were highly abundant in dormant cells, including RecA, UvrA, UvrB and UvrC. DNA repair is an important way for dormant cells to recover overall activity and potential degrading function. DNA

damage of cells was demonstrated in norfloxacin treatment, and dormant cells survived and recovered by triggering of DNA repair machinery (Hsu et al., 2006). In addition to antibiotics, other stressors can induce dormancy and trigger DNA repair, such as oxidative stress (Sikri et al., 2018), UV radiation (Murphy et al., 2006), and acidity (Murphy et al., 2003). Therefore, DNA repair, especially homologous recombination, plays important roles in bacterial dormancy transitions.

Environmental bacteria endure a complex environment in which multiple chemicals, such as antimicrobials, persistent organic pollutants, and heavy metals produce competing effects on viability and phenotype (Liu and Wong, 2013; Meng et al., 2016; Xie et al., 2019). These stressors are often studied individually, but few studies consider their co-occurrence and interaction. The present study broadened our understanding of interactions between bacterial response to antibiotics and organic pollutants, particularly biodegradation. For example, in response to environmental stress (i.e., norfloxacin exposure), ABC

transporter, one of the most common environmental information processing family proteins, was triggered to stop or reduce uptake of extracellular norfloxacin, but also nutrients and other pollutants, from moving into the cell. Many ABC transporters together with many ATP-dependent proteins were found to be less abundant in dormant cells, which was further validated by tracking decreases of ATP in the dormant cells.

The cells had to use maintenance material, such as ATP, glycogen and acetyl-CoA for continued survival under induced stress. The stress response of decreasing ABC transporter abundance and the use of intracellular ATP to maintain viability might be common for many dormancy-causing environmental factors in various bacteria (Conlon et al., 2016; Shan et al., 2017). This finding is in line with previous research that demonstrated that ATP-dependent dynamic protein aggregation regulates depth of cellular dormancy and resuscitation in persistent VBNC cells that had been induced via antibiotic and heat

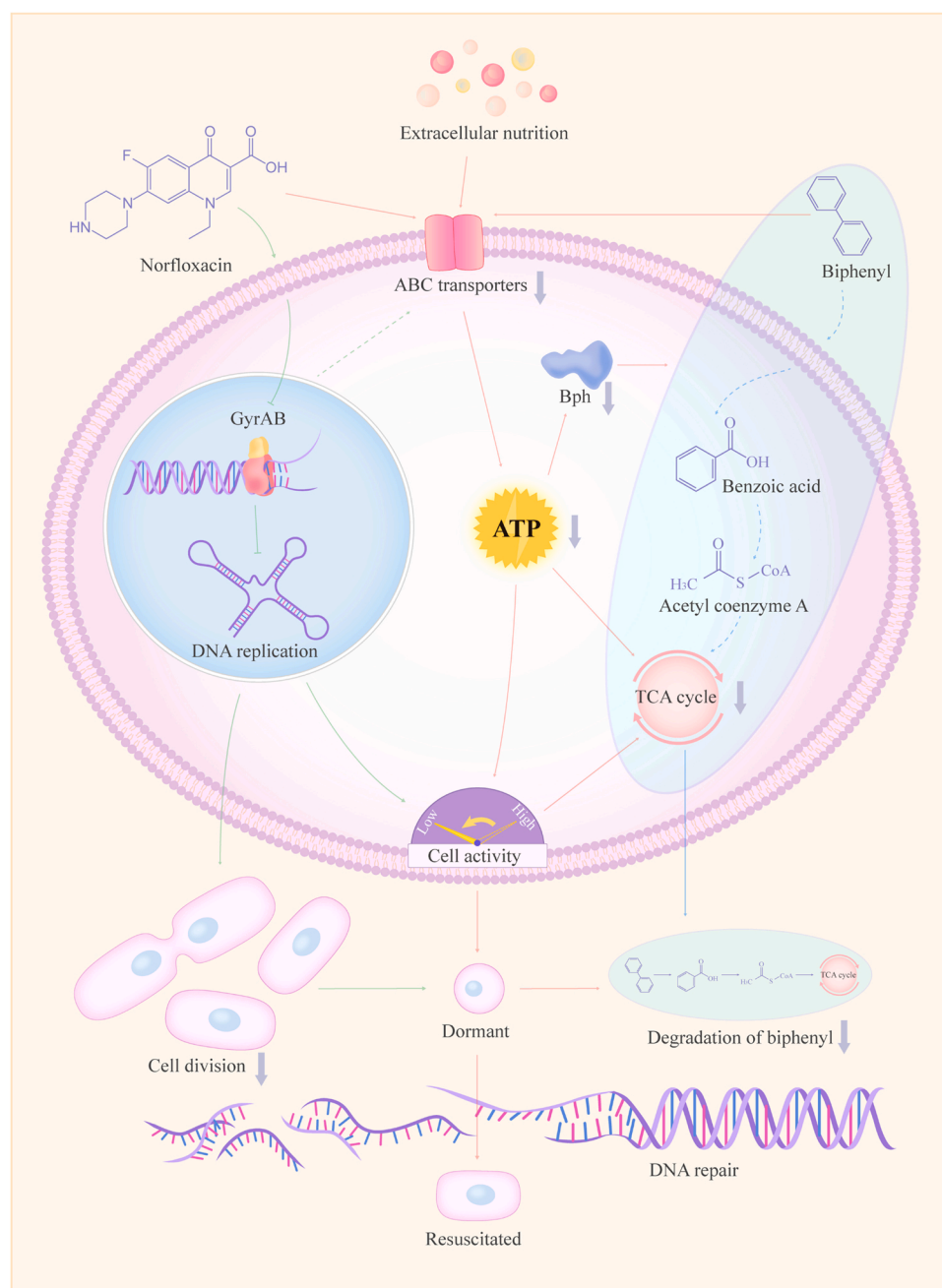


Fig. 6. Possible process of dormancy and degradation of *Rhodococcus biphenylivorans* TG9^T under the stress of norfloxacin. As a representative of environmental stress, norfloxacin would drive cell into dormant state and at the same time decrease their function of degrading. Firstly, direct response of norfloxacin treatment. Proteins involved in DNA replication, DNA damage, DNA repair were found to be differentially produced. Secondly, metabolism was decreased in the dormant cell, including the down-regulated proteins involved in ABC transporters, ATP, TCA cycle, and ribosome translation. Thirdly, lack of ATP also stopped a lot of unnecessary activity like degradation.

shock (Pu et al., 2019). Moreover, lack of ATP could also regulate the TCA cycle. The TCA cycle is an important aerobic pathway for the final steps of the oxidation of carbohydrates and fatty acids. It starts with acetyl-CoA, following a series of reactions of citrate, isocitrate, succinate, fumarate, and malate, and finally the cycle is transformed back to oxaloacetate. Our study found that TCA cycle-related proteins had significantly differential abundances, including pyruvate dehydrogenase, dihydrolipoyl dehydrogenase, acetyl-CoA, citrate synthase, isocitrate dehydrogenase, succinate dehydrogenase and malate dehydrogenase. Abundance of proteins related to the TCA cycle indicated that most metabolism in dormant cells was down-regulated, while some intracellular ATP related activity had to be triggered to maintain necessary activity.

Energy-related systems and TCA cycle are the main groups of proteins engaged in the removal of pollutants (Szewczyk et al., 2014). The TCA cycle is also a common path for bacteria to metabolism benzene-ring pollutants, which are catabolized via hydroxylated intermediates and cleavage of the benzene nucleus, followed by further degradation to cellular components and constituents of the TCA cycle (Karegoudar and Kim, 2000). As dormancy is widely occurring in bacteria under harsh conditions (Pinto et al., 2015; Ayrapetyan et al., 2018), learning and controlling bacterial dormancy could be useful for improvement of function in applications, such as resuscitating bacteria (removal of pollutants, adding Rpf protein) (Master et al., 2002; Ye et al., 2020) and avoiding or reducing dormancy (regulating dormancy at molecular level) (Pu et al., 2016, 2019).

As a surrogate of environmental stress, norfloxacin exposure drove cells into dormant state and decreased their degradation capabilities (Fig. 6). Norfloxacin inhibits formation of GyrAB-DNA complex, leaving dipolymers and single strand gaps, causing DNA damage and inhibiting DNA replication and translation. The viability and degrading activity of the existing cells were also inhibited, as well as production of new cells. To survive inhibition of DNA gyrase and the resulting DNA damage, dormant cells could trigger DNA repair to reconstruct the DNA fragment and repair damage. In addition, norfloxacin stress triggered a decrease in metabolism in the dormant cells, including the down-regulated proteins involved in ABC transporters, ATP and TCA cycle. For degrading of pollutants that contain benzene rings, the rings have to be opened and their metabolism would eventually enter the TCA cycle (Karegoudar and Kim, 2000). The down-regulation of the TCA cycle supported the observation that degradation activity was decreased in dormant cells. Also, it has been hypothesized that active transport is critically important for successful biotransformation of poorly water-soluble substrates like biphenyl and PCBs. If the ABC transporters were repressed in the dormant cells, the degradation of biphenyl and PCBs would also be decreased.

The current work aimed to advance our understanding of pathways underlying bacterial dormancy and its influence on biodegradation. Future studies should focus on validation on key proteins and pathways we uncovered. Other reported mechanisms of bacterial dormancy, including but not limited to scout hypothesis (Buerger et al., 2012; Epstein, 2009; Zalis et al., 2019), toxin and antitoxin system (Wang and Wood, 2011; Page and Peti, 2016; Harms et al., 2018), and efflux pump (Pu et al., 2016; Singh et al., 2017), may also play important roles in the dormancy transitions of strain TG9^T and should be explored.

The phenotypic variability of environmental bacteria, including survival strategies of antibiotic resistance and tolerance, plays a critical role in the fate of environmental pollutants and the potential for bioremediation. Future studies can leverage environmental degrading-bacterium *R. biphenylivorans* TG9^T, which has relatively well characterized dormancy and degradation phenotypes, as well as an experimentally verified genome annotation. We note that detection of biodegradative genes in the environment alone is insufficient to demonstrate that biodegradation is occurring explicitly because the degradation phenotype may not be expressed (Hartmann and Armen-gaud, 2014). Through evidence of the presence of proteins involved in

degradation of other organic pollutants, we surmise that TG9^T has a diversified arsenal that could be of interest for bioremediation applications.

4. Experimental procedures

4.1. Bacterial strains and growth conditions

R. biphenylivorans TG9^T (Su et al., 2015) was used in this study. This strain was isolated from a PCB-contaminated site and showed high degradation rate of PCB. Cells were routinely grown at 30 °C on nutrient agar plates or cultured in Luria-Bertani (LB) broth at 30 °C with shaking (180 rpm.).

4.2. Preparation and identification of control, dormant and resuscitated cells

Control cells were those without treatment of norfloxacin. The concentration of antibiotic needed to induce dormancy was designed according to the minimum inhibitory concentration (MIC), which was tested using a standard broth microdilution assay by Wiegand with some modification (Wiegand et al., 2008). In brief, concentration of stock solutions was 1280 mg L⁻¹. Serial two-fold dilutions of norfloxacin in Mueller-Hinton broth was spread into the 96 well-plate. The range of norfloxacin was 0.25–128 µg mL⁻¹. The final density of the bacteria for MIC test was approximately 10⁵ cfu mL⁻¹. The MIC was estimated as the lowest concentration to prevent visible growth in a certain period of time (16–24 h). To generate dormant cells, 4 mL norfloxacin (1280 mg L⁻¹) was added into 76 mL of the stock solution (turbidity at 600 nm of approximately 1) to reach a final concentration of 64 mg L⁻¹ (8 MIC) norfloxacin. Then the solutions were incubated at 30 °C, 180 rpm for 12 days. This solution was further used for cell resuscitation: the cell pellet was collected after centrifugation and washing with 0.85% NaCl buffer three times, followed by resuspension in same volume of fresh LB media and incubation for 72 h. Each day, cell viability and total cell counts of *R. biphenylivorans* TG9^T were determined using flow cytometry after staining with 5-cyano-2,3-di-(p-tolyl) tetrazolium chloride (CTC) (Molecular Probes, Eugene, OR) following the manufacturer's instructions. CTC reduced intracellularly in respiring cells to an insoluble, red fluorescent formazan precipitate. Cells not respiring or respiring at different rates will reduce different CTC and consequently produce various red fluorescent formazan product (Sieracki et al., 1999). The culturable cell number was determined by counting colonies on LB agar plates after 72 h. Preparation and morphological variations of the three states were described in our previous work (Jia et al., 2020).

4.3. Proteomics

Control, dormant, and resuscitated cells were processed using proteomics following the standard workflow previously described (Mandalakis et al., 2013). Three biological replicates were used. (i) Protein extraction. Cells were sonicated three times on ice in lysis buffer (8 M urea, 1% Protease Inhibitor Cocktail) and then the supernatant was collected by centrifugation. The concentration of the protein was further determined using BCA kit. (ii) Trypsin digestion of proteins (Sequencing Grade, Promega, porcine trypsin). The 5 mM dithiothreitol was used to reduce the protein for 30 min at 56 °C. And 11 mM iodoacetamide was added to alkylate the protein for 15 min at room temperature under dark conditions before diluting the urea concentration to less than 2 M using 100 mM Triethylammonium bicarbonate (TEAB). Finally, trypsin was added to digest the proteins for two times at different ratio (1:50, 1:100 trypsin-to-protein mass ratio). (iii) TMT labelling. Strata X C18 SPE column (Phenomenex) was used to desalt the peptides, which was further vacuum-dried (Eppendorf). Peptides were dissolved in 0.5 M TEAB and processed following the protocol of TMT kit (Thermo Fisher Scientific). (iv) Separation of peptides. The high pH reverse-phase HPLC

with an Agilent 300Extend C18 column (5 μm particles, 4.6 mm ID, 250 mm length) was used to separate the labeled peptides using a gradient of 8% to 32% acetonitrile (pH 9.0) over 60 min. Then the 60 fractions were grouped into 18 fractions before dried by vacuum centrifugation. LC-MS/MS analysis. The tryptic peptides were dissolved in 0.1% formic acid before being loaded onto a home-made reversed-phase analytical column (15-cm length, 75 μm i.d.). The gradient was comprised of an increase from 6% to 23% solvent B (0.1% formic acid in 98% acetonitrile) over 26 min, 23–35% in 8 min and climbing to 80% in 3 min then holding at 80% for the last 3 min, all at a constant flow rate of 700 nL min^{-1} on an EASY-nLC 1000 UPLC system. The peptides were subjected to NSI source followed by tandem mass spectrometry (MS/MS) in Q Exactive™ Plus (Thermo Fisher Scientific) coupled online to the UPLC. The electrospray voltage applied was 2.0 kV. The m/z scan range was 350–1800 for full scan, and intact peptides were detected in the Orbitrap at a resolution of 70,000. Peptides were then selected for MS/MS using NCE setting as 28 and the fragments were detected in the Orbitrap at a resolution of 17,500. A data-dependent acquisition (DDA) procedure was followed consisting in cycles of a MS scan followed by sequential dissociation and MS/MS scan of the 20 most abundant peptides with 15 s dynamic exclusion. Automatic gain control (AGC) was set at 5E4. Fixed first mass was set as 100 m/z .

4.4. Tandem mass spectrometry interpretation

Maxquant search engine (v.1.5.2.8) was used to process the MS/MS data. Tandem mass spectra were searched against the database which was constructed by prediction of CDS based on whole genome sequence of the strain TG9^T and concatenated with reverse decoy database with the following parameters. Trypsin/P was set as cleavage enzyme which only allowed 2 missing cleavages at most. At least one razor or unique peptide for an identification. For precursor ions, the mass tolerance was 20 ppm and 5 ppm for the First and Main search, respectively. For fragment ions, the mass tolerance was set as 0.02 Da. Then FDR (< 1%) and minimum score for peptides (>40) were set. Differentially detected proteins between two states were chosen by parameters that fold change over 1.2 or lower 1/1.2 and p value < 0.05.

The proteins were classified by Gene Ontology annotation. Identified proteins domain functional description were annotated by InterProScan based on protein sequence alignment method. KEGG database and KAAS, KEGG mapper tools were used to annotate protein pathway. CELLO was used for Subcellular localization prediction.

4.5. Protein-protein interaction

Putative protein-protein interactions were investigated to screen the important proteins and pathways involved in the process of dormancy based on statistical association. Protein-protein interaction was conducted on STRING database (Szklarczyk et al., 2019) and visualized in Cytoscape (3.7.1). In brief, all differentially produced protein sequences of three compared groups (dormant/control, resuscitated/control and resuscitated/dormant cells) were uploaded on STRING, and only interactions between the proteins belonging to the searched data set were selected, thereby excluding external candidates. STRING defines a metric called “confidence score” to define interaction confidence; we fetched all putative interactions that had a confidence score > 0.7 (high confidence). We displayed the network of protein nodes with top 100 highest degree. A graph theoretical clustering algorithm, molecular complex detection (MCODE) was utilized to analyze densely connected regions. MCODE is part of the plug-in tool kit of the network analysis and visualization software Cytoscape. Moreover, the structure of the protein RecA was predicted by SWISS-MODEL (Waterhouse et al., 2018) (<https://swissmodel.expasy.org>) and showed by PyMOL (v2.4.1).

4.6. Determination of ATP concentration in three states

The ATP contents in control, dormant and resuscitated cells were tested using an ATP Bioluminescence Assay Kit (Beyotime, S0027, China) following the manufacturer’s instructions (Pu et al., 2019). The fluorescence values of each sample were corrected to the corresponding ATP concentration based on the standard curve.

4.7. Degradation of biphenyl and PCB12

Preliminary tests showed that many congeners of PCBs could be used as the sole carbon source of *R. biphenylivorans* TG9^T (Yu et al., 2021). PCB and biphenyl has similar degradation pathway (*bph*) (Kumamaru et al., 1998; Gorbunova et al., 2021). PCB 12 was chosen as a compound representative of PCB for our assays. The control (the active TG9^T without further treatment), dormant TG9^T (the dormant TG9^T induced using norfloxacin) were collected by centrifuging at 8000 r min^{-1} for 10 min, washed three times by 0.85% NaCl, and finally suspended in mineral medium (approximately 10^5 cfu mL^{-1}). Biphenyl (1 mL, 7500 mg L^{-1}) or PCB12 (1 mL, 250 mg L^{-1}) was added and then adsorbed to the bottom of a 50 mL glass tube after evaporation of the solvent (*n*-hexane). Then, 5 mL of the prepared control and dormant TG9^T that contained the same viable cells was added into separate tubes, the cap of which was covered tightly to reduce volatilization of the medium before culturing at 30 °C, 180 r min^{-1} . The final set concentrations was 1500 mg L^{-1} and 50 mg L^{-1} of biphenyl, and PCB12, respectively. For both experiments of biphenyl and PCB12, the sterile controls were processed the same as the treated samples. The degrading rate was calculated using $\frac{C_{\text{control}} - C_{\text{TG9}}}{C_{\text{control}}} \times 100\%$. The C_{control} is the concentration of chemical in the sterile control group only contained chemical and the mineral medium without bacteria, C_{TG9} is the concentration of chemical in the treatment group which contained chemical, the mineral medium and strain TG9^T. All experiments were conducted in triplicate for each time point (12, 24, 36, 48, 60, 72 h). For each time point, 100 μL hydrochloric acid (2 mol L^{-1}) was added to the rest of the medium to stop degradation. Samples were stored at 4 °C before extraction and determination the concentration of biphenyl and PCB12.

4.8. Extraction and determination concentration of biphenyl and PCB12

Biphenyl and PCB12 was extracted according to a previous method (Tu et al., 2011). Demulsifier $(\text{NH}_4)_2\text{SO}_4$ (0.5 g) and *n*-hexane (5 mL) were added to extract the biphenyl, the tubes were sealed with tin foil, vortexed for 1 min, sonicated for 15 min before centrifuged (3000 rpm, 5 min). Then the upper organic phase was collected into a test tube and remove water by adding anhydrous Na_2SO_4 (0.4 g). Finally, the organic phase was diluted to suitable concentration by *n*-hexane before transferring approximately 1 mL for biphenyl analysis using GC-MS. 2,4,5,6-tetrachloro-*m*-xylene (TMX) and PCB209 were chosen as recovery indicators. The concentration of biphenyl was measured using a 7890A-5975 C gas chromatograph-mass spectrometer (GC-MS, Agilent Technologies Inc., USA) equipped with a DB-5 capillary column (Agilent J&W Scientific, USA). The parameters of GC programming were the same as described previously (Ye, Li et al., 2020). The average recoveries of biphenyl ($92 \pm 7.9\%$) were within the acceptable range (80–120%).

4.9. Proteogenomics analysis

A systematic six frame translation of all possible ORFs with a minimal length of 150 nucleotides was performed with the sequence manipulation suite (https://www.bioinformatics.org/sms2/orf_find.html) using the standard genetic code. The mgf files were searched against this translated ORFs database and against the annotated CDS database with the Mascot Daemon software version 2.6.1 (Matrix Science), set with the same parameters as mentioned earlier. Peptides were

identified at p value ≤ 0.05 in homology threshold mode for both databases. Those found only with the translated ORFs database were retained. Translated ORFs identified with at least two of these peptides were systematically analyzed by BLAST against the NCBI nr protein sequence database for N-terminal structure determination and function annotation based on consensus information as previously reported (Hartmann and Armengaud, 2014).

CRedit authorship contribution statement

Chaofeng Shen: Supervised the study. **Erica Marie Hartmann:** Supervised the study. **Chungui Yu:** Designed the research, Analyzed the data, Wrote the paper, Performed the experiments. **Jean Armengaud:** Analyzed the data, Wrote the paper. **Jean-Charles Gaillard:** Analyzed the data, Helped modify the manuscript. **Ryan Andrew Blaustein:** Wrote the paper. **Kezhen Chen:** Performed the experiments. **Zhe Ye:** Performed the experiments. **Fengjun Xu:** Performed the experiments. **Zhihui Qin:** Helped modify the manuscript. **Yulong Fu:** Helped modify the manuscript. All authors read and approved the final manuscript.

Declaration of Competing Interest

The authors declare that they have no known competing financial interests or personal relationships that could have appeared to influence the work reported in this paper.

Acknowledgments

This study was supported by the National Key Research and Development Plan (2019YFC1803700), National Natural Science Foundation of China (21876149, 42077125).

Appendix A. Supporting information

Supplementary data associated with this article can be found in the online version at doi:10.1016/j.jhazmat.2021.127712.

References

- Adriaens, P., Focht, D.D., 1990. Continuous coculture degradation of selected polychlorinated biphenyl congeners by *Acinetobacter* spp. in an aerobic reactor system. *Environ. Sci. Technol.* 24, 1042–1049.
- Al-Bana, B.H., Haddad, M.T., Garduno, R.A., 2014. Stationary phase and mature infectious forms of *Legionella pneumophila* produce distinct viable but non-culturable cells. *Environ. Microbiol.* 16, 382–395.
- Ayrapetyan, M., Williams, T., Oliver, J.D., 2018. Relationship between the viable but nonculturable state and antibiotic persister cells. *J. Bacteriol.* 200 (20), e00249–18.
- Baker, S., Thomson, N., Weill, F.X., Holt, K.E., 2018. Genomic insights into the emergence and spread of antimicrobial-resistant bacterial pathogens. *Science* 360, 733–738.
- Blaustein, R.A., McFarland, A.G., Ben Maamar, S., Lopez, A., Castro-Wallace, S., Hartmann, E.M., 2019. Pangenomic approach to understanding microbial adaptations within a model built environment, the international space station, relative to human hosts and soil. *Msystems*. 4 (1) e00281-18.
- Boonsaner, M., Hawker, D.W., 2010. Accumulation of oxytetracycline and norfloxacin from saline soil by soybeans. *Sci. Total Environ.* 408, 1731–1737.
- Brauner, A., Fridman, O., Gefen, O., Balaban, N.Q., 2016. Distinguishing between resistance, tolerance and persistence to antibiotic treatment. *Nat. Rev. Microbiol.* 14, 320–330.
- Buerger, S., Spoering, A., Gavriš, E., Leslin, C., Ling, L., Epstein, S.S., 2012. Microbial scout hypothesis, stochastic exit from dormancy, and the nature of slow growers. *Appl. Environ. Microbiol.* 78, 3221–3228.
- Carvalho, V., Perez-Cabezas, B., Oliveira, C., Vitorino, R., Vilanova, M., Cerca, N., 2018. Tetracycline and rifampicin induced a viable but nonculturable state in *Staphylococcus epidermidis* biofilms. *Future Microbiol.* 13, 27–36.
- Conlon, B.P., Rowe, S.E., Gandt, A.B., Nuxoll, A.S., Donegan, N.P., Zalis, E.A., Clair, G., Adkins, J.N., Cheung, A.L., Lewis, K., 2016. Persister formation in *Staphylococcus aureus* is associated with ATP depletion. *Nat. Microbiol.* 1, 16051.
- Dai, H.H., Gao, J.F., Li, D.C., Wang, Z.Q., Duan, W.J., 2021. Metagenomics combined with DNA-based stable isotope probing provide comprehensive insights of active trichloro- degrading bacteria in wastewater treatment. *J. Hazard. Mater.* 404 (PtB), 124192.
- Epstein, S.S., 2009. Microbial awakenings. *Nature*. 457 (7233), 1083.

- Gorbunova, T.I., Egorova, D.O., Pervova, M.G., Kyrianova, T.D., Demakov, V.A., Saloutin, V.I., Saloutin, V.I., Chupakhin, O.N., 2021. Biodegradation of trichlorobiphenyls and their hydroxylated derivatives by *Rhodococcus*-strains. *J. Hazard. Mater.* 409, 124471.
- Harms, A., Brodersen, D.E., Mitarai, N., Gerdes, K., 2018. Toxins, targets, and triggers: an overview of toxin-antitoxin biology. *Mol. Cell.* 70, 768–784.
- Hartmann, E.M., Armengaud, J., 2014. Shotgun proteomics suggests involvement of additional enzymes in dioxin degradation by *Sphingomonas wittichii* RW1. *Environ. Microbiol.* 16, 162–176.
- Hsu, Y.H., Chung, M.W., Li, T.K., 2006. Distribution of gyrase and topoisomerase IV on bacterial nucleoid: implications for nucleoid organization. *Nucleic Acids Res.* 34, 3128–3138.
- Jia, Y., Yu, C., Fan, J., Fu, Y., Ye, Z., Guo, X., Xu, Y., Shen, C., 2020. Alterations in the cell wall of *Rhodococcus biphenylivorans* under norfloxacin stress. *Front. Microbiol.* 11, 554957.
- Karegoudar, T.B., Kim, C.K., 2000. Microbial degradation of monohydroxybenzoic acids. *J. Microbiol.* 38, 53–61.
- Klein, E.Y., Van Boeckel, T.P., Martinez, E.M., Pant, S., Gandra, S., Levin, S.A., Goossens, H., Laxminarayan, R., 2018. Global increase and geographic convergence in antibiotic consumption between 2000 and 2015. *Proc. Natl. Acad. Sci. USA*. 115, E3463–E3470.
- Kumamaru, T., Suenaga, H., Mitsuoka, M., Watanabe, T., Furukawa, K., 1998. Enhanced degradation of polychlorinated biphenyls by directed evolution of biphenyl dioxygenase. *Nat. Biotechnol.* 16, 663–666.
- Le, T.X., Munkage, Y., Kato, S., 2005. Antibiotic resistance in bacteria from shrimp farming in mangrove areas. *Sci. Total Environ.* 349, 95–105.
- Levy, S.B., Marshall, B., 2004. Antibacterial resistance worldwide: causes, challenges and responses. *Nat. Med.* 10, S122–S129.
- Lewis, K., Shan, Y., 2017. Why tolerance invites resistance bacteria that encounter antibiotics first become tolerant and then resistant to them. *Science*. 355, 796, 796–796.
- Liu, J.L., Wong, M.H., 2013. Pharmaceuticals and personal care products (PPCPs): a review on environmental contamination in China. *Environ. Int.* 59, 208–224.
- Liu, X., Steele, J.C., Meng, X.Z., 2017. Usage, residue, and human health risk of antibiotics in Chinese aquaculture: a review. *Environ. Pollut.* 223, 161–169.
- Louvado, A., Gomes, N.C., Simoes, M.M., Almeida, A., Cleary, D.F., Cunha, A., 2015. Polycyclic aromatic hydrocarbons in deep sea sediments: microbe-pollutant interactions in a remote environment. *Sci. Total Environ.* 526, 312–328.
- Mandalakis, M., Panikov, N., Dai, S., Ray, S., Karger, B.L., 2013. Comparative proteomic analysis reveals mechanistic insights into *Pseudomonas putida* F1 growth on benzoate and citrate. *AMB Express*. 3 (1), 64.
- Master, E.R., Lai, V.W.M., Kuipers, B., Cullen, W.R., Mohn, W.W., 2002. Sequential anaerobic-aerobic treatment of soil contaminated with weathered aroclor 1260. *Environ. Sci. Technol.* 36, 100–103.
- Meng, X.Z., Venkatesan, A.K., Ni, Y.L., Steele, J.C., Wu, L.L., Bignert, A., Bergman, Å., Halden, R.U., 2016. Organic contaminants in Chinese sewage sludge: a meta-analysis of the literature of the past 30 years. *Environ. Sci. Technol.* 50, 5454–5466.
- Meredith, H.R., Srimani, J.K., Lee, A.J., Lopatkin, A.J., You, L., 2015. Collective antibiotic tolerance: mechanisms, dynamics and intervention. *Nat. Chem. Biol.* 11, 182–188.
- Murphy, C., Carroll, C., Jordan, K.N., 2003. Induction of an adaptive tolerance response in the foodborne pathogen, *Campylobacter jejuni*. *Fems Microbiol. Lett.* 223 (1), 89–93.
- Murphy, C., Carroll, C., Jordan, K.N., 2006. Environmental survival mechanisms of the foodborne pathogen *Campylobacter jejuni*. *J. Appl. Microbiol.* 100, 623–632.
- Neu, H.C., 1992. The crisis in antibiotic resistance. *Science*. 257, 1064–1073.
- Oliver, J.D., 1995. The viable but non-culturable state in the human pathogen *Vibrio vulnificus*. *Fems Microbiol. Lett.* 133, 203–208.
- Page, R., Peti, W., 2016. Toxin-antitoxin systems in bacterial growth arrest and persistence. *Nat. Chem. Biol.* 12, 208–214.
- Pasquaro, S., Zandri, G., Vignaroli, C., Vuotto, C., Donelli, G., Biavasco, F., 2013. Antibiotic pressure can induce the viable but non-culturable state in *Staphylococcus aureus* growing in biofilms. *J. Antimicrob. Chemother.* 68, 1812–1817.
- Pinto, D., Santos, M.A., Chambel, L., 2015. Thirty years of viable but nonculturable state research: unsolved molecular mechanisms. *Crit. Rev. Microbiol.* 41, 61–76.
- Pu, Y., Li, Y., Jin, X., Tian, T., Ma, Q., Zhao, Z., Lin, S.Y., Chen, Z., Li, B., Yao, G., Leake, M.C., Lo, C.J., Bai, F., 2019. ATP-dependent dynamic protein aggregation regulates bacterial dormancy depth critical for antibiotic tolerance. *Mol. Cell.* 73, 143–156.
- Pu, Y., Zhao, Z., Li, Y., Zou, J., Ma, Q., Zhao, Y., Ke, Y., Zhu, Y., Chen, H., Baker, M., Ge, H., Sun, Y., Xie, X.S., Bai, F., 2016. Enhanced efflux activity facilitates drug tolerance in dormant bacterial cells. *Mol. Cell.* 62, 284–294.
- Ryu, A.R., Mok, J.S., Lee, D.E., Kwon, J.Y., Park, K., 2019. Occurrence, virulence, and antimicrobial resistance of *Vibrio parahaemolyticus* isolated from bivalve shellfish farms along the southern coast of Korea. *Environ. Sci. Pollut. Res.* 26, 21034–21043.
- Shan, Y., Brown Gandt, A., Rowe, S.E., Deisinger, J.P., Conlon, B.P., Lewis, K., 2017. ATP dependent persister formation in *Escherichia coli*. *Mbio*. 8 (1), e02267-16.
- Shen, L.L., Pernet, A.G., 1985. Mechanism of inhibition of DNA gyrase by analogs of nalidixic acid: the target of the drugs is DNA. *Proc. Natl. Acad. Sci. USA*. 82, 307–311.
- Sieracki, M.E., Cucci, T.L., Nicinski, J., 1999. Flow cytometric analysis of 5-cyano-2,3-ditolyl tetrazolium chloride activity of marine bacterioplankton in dilution cultures. *Appl. Environ. Microbiol.* 65, 2409–2417.
- Sikri, K., Duggal, P., Kumar, C., Batra, S.D., Vashist, A., Bhaskar, A., Tripathi, K., Sethi, T., Singh, A., Tyagi, J.S., 2018. Multifaceted remodeling by vitamin C boosts

- sensitivity of *Mycobacterium tuberculosis* subpopulations to combination treatment by anti-tubercular drugs. *Redox Biol.* 15, 452–466.
- Singh, S., Kalia, N.P., Joshi, P., Kumar, A., Sharma, P.R., Kumar, A., Bharate, S.B., Khan, I.A., 2017. Boeravinone B, a novel dual inhibitor of NorA bacterial efflux pump of *Staphylococcus aureus* and human P-Glycoprotein, reduces the biofilm formation and intracellular invasion of bacteria. *Front. Microbiol.* 8, 1868.
- Su, X., Liu, Y., Hashmi, M.Z., Hu, J., Ding, L., Wu, M., Shen, C., 2015. *Rhodococcus biphenylivorans* sp. nov., a polychlorinated biphenyl-degrading bacterium. *Antonie Van Leeuwenhoek.* 107, 55–63.
- Szewczyk, R., Sobon, A., Sylwia, R., Dzitko, K., Waidelich, D., Dlugonski, J., 2014. Intracellular proteome expression during 4-n-nonylphenol biodegradation by the filamentous fungus *Metarhizium robertsii*. *Int. Biodeterior. Biodegrad.* 93, 44–53.
- Szklarczyk, D., Gable, A.L., Lyon, D., Junge, A., Wyder, S., Huerta-Cepas, J., Simonovic, M., Doncheva, N.T., Morris, J.H., Bork, P., Jensen, L.J., Mering, C.V., 2019. STRING v11: protein-protein association networks with increased coverage, supporting functional discovery in genome-wide experimental datasets. *Nucleic Acids Res.* 47, D607–D613.
- Tu, C., Teng, Y., Luo, Y., Li, X., Sun, X., Li, Z., Liu, W., Christie, P., 2011. Potential for biodegradation of polychlorinated biphenyls (PCBs) by *Sinorhizobium meliloti*. *J. Hazard Mater.* 186 (2–3), 1438–1444.
- Tymensen, L., Booker, C.W., Hannon, S.J., Cook, S.R., Jokinen, C.C., Zaheer, R., Read, R., Boerlin, P., McAllister, T.A., 2019. Plasmid distribution among *Escherichia coli* from livestock and associated wastewater: unraveling factors that shape the presence of genes conferring third-generation cephalosporin resistance. *Environ. Sci. Technol.* 53, 11666–11674.
- Viancelli, A., Michelon, W., Rogovski, P., Cadamuro, R.D., de Souza, E.B., Fongaro, G., Camargo, A.F., Stefanski, F.S., Venturin, B., Scapini, T., Bonatto, C., Preczeski, K.P., Klanovicz, N., de Oliveira, D., Treichel, H., 2020. A review on alternative bioprocesses for removal of emerging contaminants. *Bioprocess Biosyst. Eng.* 43, 2117–2129.
- Wang, F., Gao, J., Zhai, W., Cui, J., Liu, D., Zhou, Z., Wang, P., 2021. Effects of antibiotic norfloxacin on the degradation and enantio selectivity of the herbicides in aquatic environment. *Ecotoxicol. Environ. Saf.* 208, 111717.
- Wang, X., Wood, T.K., 2011. Toxin-antitoxin systems influence biofilm and persister cell formation and the general stress response. *Appl. Environ. Microbiol.* 77, 5577–5583.
- Waterhouse, A., Bertoni, M., Bienert, S., Studer, G., Tauriello, G., Gumienny, R., Gumienny, R., Heer, F.T., de Beer, T., Rempfer, C., Bordoli, L., Lepore, R., Schwede, T., 2018. SWISS-MODEL: homology modelling of protein structures and complexes. *Nucleic Acids Res.* 46 (W1), W296–W303.
- Whitesides, M.D., Oliver, J.D., 1997. Resuscitation of *Vibrio vulnificus* from the viable but nonculturable state. *Appl. Environ. Microbiol.* 63, 1002–1005.
- Wiegand, I., Hilpert, K., Hancock, R.E., 2008. Agar and broth dilution methods to determine the minimal inhibitory concentration (MIC) of antimicrobial substances. *Nat. Protoc.* 3, 163–175.
- Xie, H., Hao, H., Xu, N., Liang, X., Gao, D., Xu, Y., Gao, Y., Tao, H., Wong, M., 2019. Pharmaceuticals and personal care products in water, sediments, aquatic organisms, and fish feeds in the Pearl River Delta: occurrence, distribution, potential sources, and health risk assessment. *Sci. Total Environ.* 659, 230–239.
- Ye, Z., Li, H., Jia, Y., Fan, J., Wan, J., Guo, L., Su, X., Zhang, Y., Wu, W.M., Shen, C., 2020. Supplementing resuscitation-promoting factor (Rpf) enhanced biodegradation of polychlorinated biphenyls (PCBs) by *Rhodococcus biphenylivorans* strain TG9^T. *Environ. Pollut.* 263, 114488, 114488–114488.
- Yu, C., Wang, H., Blaustein, R.A., Guo, L., Ye, Q., Fu, Y., Fan, J., Su, X., Hartmann, E.M., Shen, C., 2021. Pangenomic and functional investigations for dormancy and biodegradation features of an organic pollutant-degrading bacterium *Rhodococcus biphenylivorans* TG9. *Sci. Total Environ.*, 151141
- Zalis, E.A., Nuxoll, A.S., Manuse, S., Clair, G., Radlinski, L.C., Conlon, B.P., Adkins, J., Lewis, K., 2019. Stochastic variation in expression of the tricarboxylic acid cycle produces persister cells. *Mbio.* 10 (5), e01930–19.
- Zhang, J., Wang, L., Shi, L., Chen, X., Chen, C., Hong, Z., Cao, Y., Zhao, L., 2020. Survival strategy of *Cronobacter sakazakii* against ampicillin pressure: induction of the viable but nonculturable state. *Int. J. Food Microbiol.* 334, 108819, 108819–108819.
- Zhang, R., Kang, Y., Zhang, R., Han, M., Zeng, W., Wang, Y., Yu, K., Yang, Y., 2021. Occurrence, source, and the fate of antibiotics in mariculture ponds near the Maowei Sea, South China: storm caused the increase of antibiotics usage. *Sci. Total Environ.* 752, 141882, 141882–141882.
- Zhu, Y.G., Johnson, T.A., Su, J.Q., Qiao, M., Guo, G.X., Stedtfeld, R.D., Hashsham, S.A., Tiedje, J.M., 2013. Diverse and abundant antibiotic resistance genes in Chinese swine farms. *Proc. Natl. Acad. Sci. USA.* 110, 3435–3440.